Available online at www.sciencedirect.com

ScienceDirect

IFAC PapersOnline CONFERENCE PAPER ARCHIVE

IFAC PapersOnLine 53-2 (2020) 16031–16036

Pulse Wave Velocity Measurement in the Carotid Artery Using an LED-LED Array Pulse Oximeter ⋆

Jake D. Campbell * **Lui Holder-Pearson** *
Christopher G. Pretty * **Phil Bones** ** **J. Geoffrey Chase** *

* *Mechanical Engineering Department, University of Canterbury, Christchurch, New Zealand (e-mail: jake.campbell@pg.canterbury.ac.nz).*
** *Electrical Engineering Department, University of Canterbury, Christchurch, New Zealand.*

Abstract:
Pulse wave velocity (PWV) is frequently used as an early indicator of risk of cardiovascular disease. Conventional methods of PWV measurement are invasive and measure the regional PWV, introducing errors from unknown measurement distance to masking local changes in compliance. This paper describes the development and testing of a non-invasive PWV sensor using photoplethysmograph signals. The sensor measures the pulse in the carotid artery with three sensor arrays spaced at 20 mm, 30 mm and 50 mm spacing. Each array of 20 LED-LED sensors are placed at 5 mm to get the largest amplitude pulse across the neck, and to allow for inaccurate sensor placement. LEDs are used as light emitters and the inherent capacitance of reverse biased LEDs measure the reflected light. The foot-foot and phase difference methods were used to calculate the PWV at each measurement distance. The foot-foot method was more reliable than the phase difference at all distances with a PWV of 5.26 $\mathrm{m\,s^{-1}}$ in a single-subject trial. The sample rate of 570 Hz was deemed too slow as one sample difference resulted in a PWV change of 1.5 $\mathrm{m\,s^{-1}}$. The developed sensor measured the local PWV within the expected physiological range around 6 $\mathrm{m\,s^{-1}}$. All future measurements will be measured at 1 kHz and an increased LED output intensity.

Keywords: Pulse wave velocity, non-invasive, photoplethysmography, LED-LED detection, carotid artery

1. INTRODUCTION

Cardiovascular disease is a leading cause of death, responsible for an estimated 30% of deaths (Mendis, 2015). Many methods for early risk detection have been investigated, with arterial pulse wave velocity being an indicator of changing blood pressure, as well as early detection of the onset of sepsis (Kazune et al., 2014; Kadoglou et al., 2012). Pulse wave velocity (PWV) is used to indicate arterial stiffness, with risk of health complications increasing with higher stiffness levels (Peter et al., 2015; Pereira et al., 2015). The physiological range for PWV increases with age from 6 $\mathrm{m\,s^{-1}}$ below 30 years old, to 11 $\mathrm{m\,s^{-1}}$ over 70 years old (Boutouyrie and Vermeersch, 2010).

This paper presents a new sensor placed on the neck to extract the patients PWV. Photoplethysmograph signals are measured at three distances along the neck to detect the pulse in the carotid artery. Two signal processing methods are tested to determine the most accurate method for this sensor (foot-foot, phase difference).

1.1 Measuring Sites

During systolic cardiac contraction a pressure wave propagates along the arterial tree. As it travels from large arteries to the peripheries, the speed of the wave changes due to the increase in arterial compliance further from the heart (Janić et al., 2014). Measurement of the effective PWV from the carotid to femoral artery is considered the gold standard (Laurent et al., 2006). Carotid-femoral PWV is a metric of PWV corresponding to the widely accepted arterial propagation mode.

For reliable measurement of PWV, the same point of each pulse wave must be found for comparison. Traditionally, the foot-foot method is used. The foot of the waveform signifies the start of systole and is the point of the wave minimally affected by the reflection wave (Segers et al., 2009). Figure 1 illustrates the method. The distance between sites is critical to accurate calculation of PWV. The distance can be directly measured (dual lumen pressure catheter through the aorta) or obtained by subtracting the carotid measurement site to sternal notch distance from the sternal notch to femoral measurement site distance. Different distance measurement techniques can result in PWV values varying by up to 30% (Salvi et al., 2008).

⋆ The project has received funding from EU H2020 R&I programme (MSCA-RISE-2019 call) under agreement #872488 –DCPM

10.1016/j.ifacol.2020.12.406

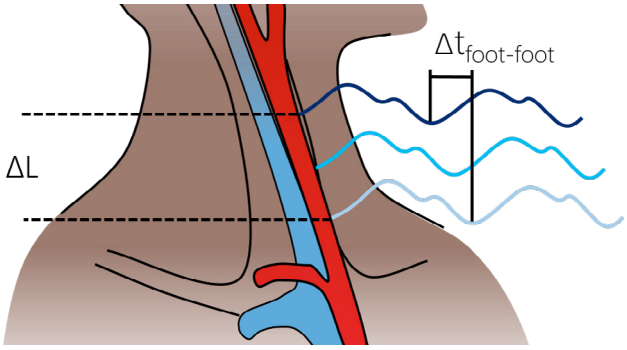

Fig. 1. Foot to foot PWV method.

An additional method is to use the intersecting tangent algorithm, which finds the site of the steepest slope during systole.

PWV measured across different vessels, such as carotid-femoral and carotid-radial, are considered regional measurements, where the calculated PWV is the average over different arteries with varying compliance (Boutouyrie et al., 2009). Consequently, regional PWV may mask changes in compliance in small segments. The regional PWV is defined by the distance between measurement points and the pulse transit time (PTT) delay between the two points (Pereira et al., 2015). This relationship is shown in Equation 1. Another potential pitfall of regional sensing is the distance the pulse wave travels includes the vascular curvature, increasing areas of error. Commercial devices measuring the regional PWV, such as PulsePen and SphygmoCor, must make assumptions for these effects.

$$PWV = \frac{d_{carotid-femoral}}{PTT} \tag{1}$$

Previous attempts at non-invasive PWV measurement have used the start of the R wave of the ECG signals to indicate the start of the pulse wave at the carotid artery(Balmer et al., 2017). However, it was determined that ECG does not provide a reliable substitute as the start of the R wave occurs before blood is ejected, so adds an offset to the time delay that is very variable within and between subjects. Thus, it was recommended to investigate local PWV signals without using ECG.

The designed sensor uses a different method for calculating the time difference between pulses. Rather than only take the difference at certain points on the wave (foot-foot), the phase difference across consecutive waves was also calculated. By subtracting the phase over a longer period of time, the average PWV is estimated. For regional PWV, this method was found to be negatively influenced by the reflectance wave (Bertram et al., 1997; Segers et al., 2009). However, this effect is expected to be minimised in local measurement with only 50 mm between detectors.

1.2 Existing Sensors

While regional PWV is considered the gold standard measurement for arterial stiffness, local PWV measurement on a single artery has been investigated. Hsu et el developed a PWV sensor capable of being placed on either the radial or

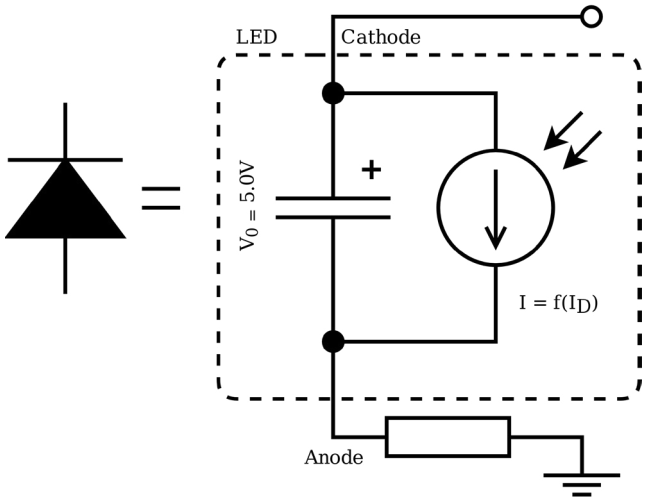

Fig. 2. Circuit diagram for the LED-LED detection method.

the carotid artery (Hsu and Young, 2014). Their approach used two packaged silicone-coated microelectromechanical sensors (MEMS) pressure sensors. Results from this sensor gave an average PWV of 5.1 m s^{-1} on the neck, inline with the expected carotid PWV in healthy patients (Janić et al., 2014). Another paper by (Fabian et al., 2019) compared the brachial occlusion-cuff technique to a SphygmoCor VX, gaining a correlation of r = 0.88 (p ¡ 0.001).

Peter et al. (2015) developed a dual channel photoplethysmograph sensor with sensors placed 60 mm apart, but temporal resolution was deemed insufficient to accurately measure PWV. Sorensen et al. (2008)determined with a variable sampling-speed resolution, that the same results for PWV were able to be determined both at sample rates of 4 kHz and 1 kHz. Therefore exceeding this sample rate does not seem to have additional benefit.

1.3 LED-LED Light Detection

In a conventional pulse oximeter, an LED is used to emit light and a photodiode detects the returning light. The proportional change in photodiode current to the intensity of light detected by the sensor is amplified, converted to a voltage, then sampled through an analog to digital converter (ADC) (Kennedy, 2015). While this circuitry is useful for singular detection points, incorporation into a high resolution, multisensor array requires a complicated setup of LED driving circuits and analog electronics (Shen et al., 2010).

Rather than use a photodiode as a light detector, a reverse-biased LED is used to detect light. This approach does not take instantaneous measurements with an ADC, the detecting LED uses its inherent capacitance to integrate the incoming light intensity over the sensing period (Stojanovic and Karadaglic, 2013; Lau et al., 2006). An equivalent circuit diagram for the reverse-biased LED can be seen in Figure 2. Work by Lau et al. (2006) demonstrated LED detection yields an order of magnitude increase in sensitivity to changes in light intensity compared to photodiodes. A further benefit of LED detection is the narrow wavelength detection range, meaning the LED has bet-

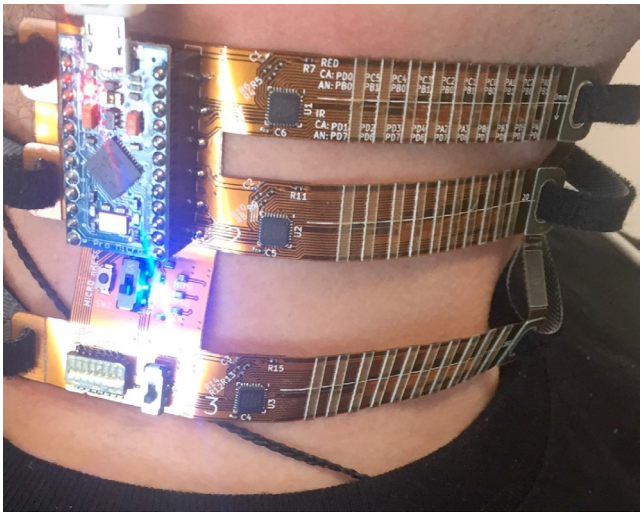

Fig. 3. Example placement of sensor on neck.

ter response to light in the wavelength areas of interest (O'Toole and Diamond, 2008).

2. METHODS

To measure the PWV through the carotid artery, a sensor with 60 LEDs was built. Three arrays with 20 LEDs were used to measure the pulse at different points along the carotid artery. Each wavelength to be detected had a pair of LEDs. One emitting and the other detecting the reflected light. By connecting the anode and cathode of each LED to the micro-controller pins, the circuit complexity is minimised.

2.1 Sensor Design

Figure 4 shows the LED layout on the designed board. Each array is controlled by an ATtiny88 micro-controller. As the system uses LEDs to both emit and detect light using time, the complexity of the system is significantly reduced compared to using photodiodes. This micro-controller was chosen as it has 32 GPIO pins required to control the LEDs. The inbuilt ATtiny clock runs at 8 MHz, with a temporal resolution of two CPU clock counts correlating to a timing resolution of 250 ns. The ATtinys were programmed with AtmelStudio 7.0 and the data collected and analysed in MATLAB R2019.

The LEDs used in this project are from the SunLED pulse oximeter series (XZM2MRTNI55W-8). These LEDs were chosen as the red (660 nm) and infrared (940 nm) LEDs are contained in one package, reducing footprint size. By having the red and infrared LEDs, the sensor is also capable of arterial oxygen saturation (S_AO_2) monitoring. An Arduino Pro Micro is used as the serial interface to the PC and communicates to each ATtiny through SPI. During each measurement cycle, an LED is designated the emitter and the adjacent one the detector.

Each LED package is separated by 5 mm, allowing measurement at either adjacent positions or 10 mm apart. By placing each LED package in an array, the sensor does not need to be placed accurately over the carotid artery, as the largest pulse amplitude across each array is used for PWV

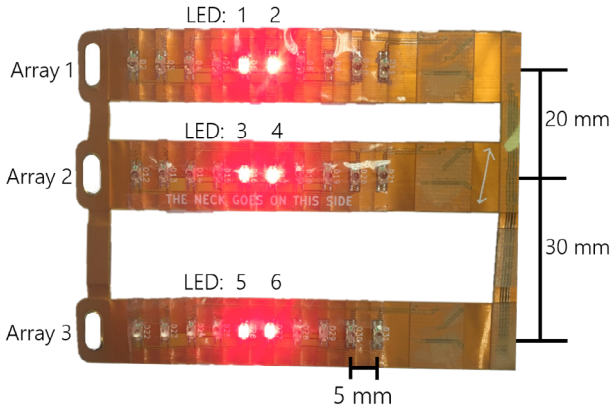

Fig. 4. LED layout of the flexible PWV board.

measurement, thereby effectively finding the carotid artery in real-time. The hypotenuse between detecting LEDs is taken as the pulse travel distance. To ensure maximum contact with the neck, the sensor is flexible. The end of each array is attached to a velcro strap to hold the board onto the neck with minimum pressure as per Figure 3.

As previous methods of PWV detection use between 20 mm and 60 mm reading distances (Peter et al., 2015; Sorensen et al., 2008), the sensor was constructed with reading distances of 20 mm, 30 mm and 50 mm. These three array spacings are shown in Figure 4. At these distances, for an expected PWV of 5 m s^{-1}, the delay times are expected to range from 4 ms at 20 mm and 10 ms at 50 mm.

The ATtiny drives the LEDs at 2.1 V (red) and 1.2 V (infrared), with current limiting resistors of 60 Ω (red) and 105 Ω (infrared) for a drive current of 20 mA. Figure 5 shows the detection sequence used by each LED. The detector LED is reverse biased (charged) for 100 µs and the emitter LED is turned on. After charging, the cathode pin of the ATtiny88 is switched to high impedance. The time taken for the voltage across the LED to drop from logic high (3.3 V) to logic low (1.3 V) is recorded.

3. SENSOR TESTING

The sensor was run at 570 Hz, with each array making two readings in this time (6 total readings). While the sensor is capable of making the 6 measurements at 1 kHz, in this testing the serial communications limited the data transfer to 570 Hz. The two largest pulsatile signals for each array were identified and were used throughout the testing. Validating the sensor is difficult without invasive measurements. Testing was completed on one subject for five beats. The sensor was held onto the neck with Velcro straps.During the test the patient held their breath to minimise the variation due to respiration.

The foot-foot and phase detection algorithms were used over each of the distance values where signals from LED 1 and 2 were at 0 mm (array 1), signals from LEDs 3 and 4 at 20 mm (array 2) and signals from LEDs 5 and 6 at 50 mm (array 3). Each LED is sequentially measured and each measurement takes 0.3 ms. This is done to remove the effect of light from other arrays affecting another. As 6 measurements are taken within the 1.75 ms (570 Hz)

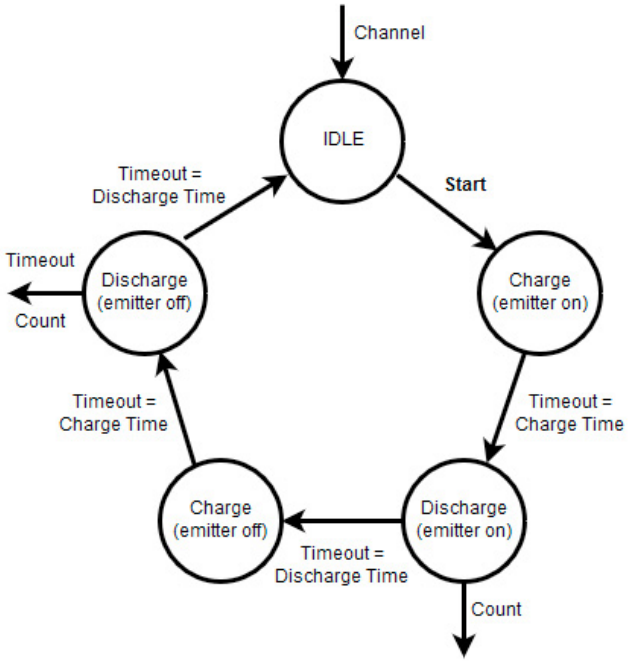

Fig. 5. Finite state machine for a sensing cycle.

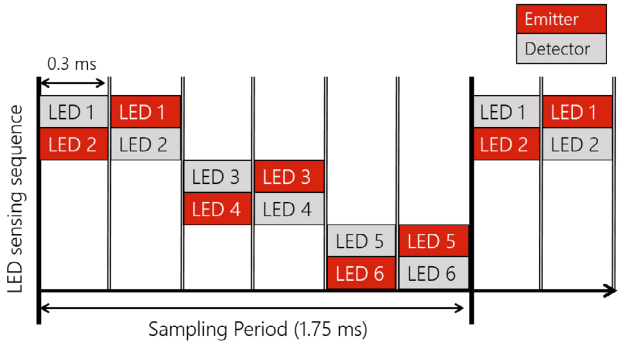

Fig. 6. Timing diagram over the sampling period.

sampling period, the time delay between each reading (0.3 ms) is included in the PWV calculation. This is shown in Figure 6.

There are four PWV readings for each distance. For 50 mm the readings are between: LED 1 to LED 5, LED 1 to LED 6, LED 2 to LED 5 and LED 2 to LED 6. These four readings are averaged to get the PWV at 50 mm. The process is repeated for 20 mm and 30 mm.

4. RESULTS

4.1 Sensor Response

With the sensor placed on the neck as shown in Figure 3, the 5^{th} and 6^{th} LEDs in each array gave the strongest pulse amplitudes. The data from these LEDs are shown in Figure 7. Each time series was filtered with a 15 Hz cut off low-pass butterworth IIR filter.

During testing it was found that the sensor gave the largest signals with the sensor orientation inverted, so the 0 mm and 20 mm arrays were placed closer to the heart. This orientation is seen in Figure 7 as the pulse amplitudes

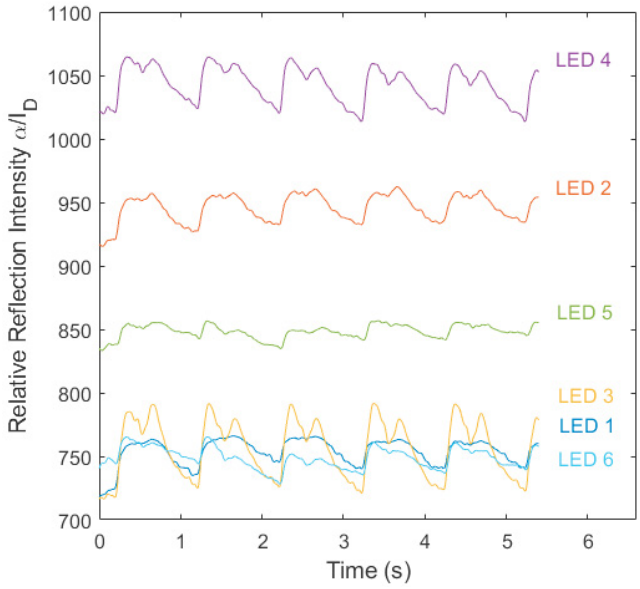

Fig. 7. Pulse amplitudes in the carotid artery at 0 mm (LED 1 and 2), 20 mm (LED 3 and 4) and 50 mm (LED 5 and 6).

of the 50 mm array (LED 5 and 6) are smaller than the other two arrays. The relative reflection intensity in Figure 7 represents the amount of light absorbed in the tissue. During systole, there is more blood present in the path length so more light is absorbed. As the LEDs integrate the reflected light intensity, greater light absorption is represented by a longer LED discharge time.

The measurement time for each LED was limited to below 256 µs to ensure a sample rate of 570 Hz. The relative reflection intensity is measured in the time taken for the LED to discharge. This is represented in clock counts along the y axis of Figure 7. The amplitude of each LED pulse in Figure 7 ranges from 12 clock counts (LED 5) to 70 clock counts (LED 3) with a resolution of 2 clock counts. For the strongest signal, the sensor is held against the neck by the strap with only the force required to stop motion artefacts.

4.2 Foot-foot Method

The systole present in Figure 7 at 4.2 s was used or foot-foot analysis. Figure 8 plots the systole present in LED 1 and LED 6. As shown in the plot, there is a time delay present of 11 ms. Accounting for the 1.45 ms delay between LED 1 and LED 6 reading (shown in Figure 6), Equation 2 gives a pulse wave velocity of $5.26ms^{-1}$. This result is within the expected PWV range given by Boutouyrie et el (Boutouyrie and Vermeersch, 2010).

$$PWV = \frac{0.05}{(0.011 - 0.00145)} = 5.26ms^{-1} \qquad (2)$$

4.3 Phase Difference Method

The phase difference method was run over the same data as the foot-foot method. Table 1 compares the phase differences between the LEDs to the foot-foot method. The

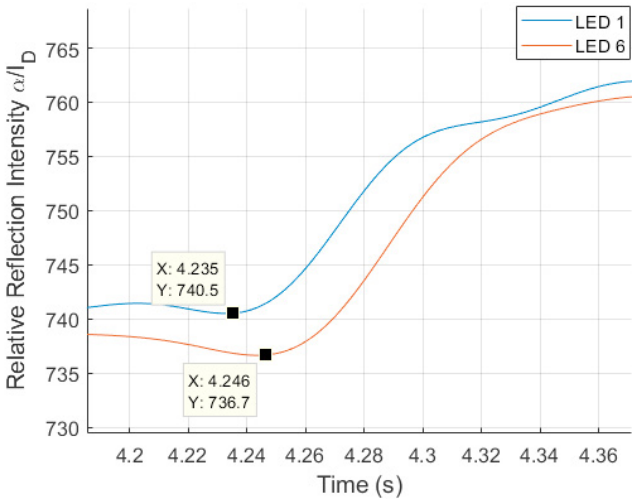

Fig. 8. Foot-foot pulse transit time between LED 1 and LED 6.

Table 1. Comparison between foot-foot PWV and the phase detection PWV method for different LED reading distances.

	LEDs	Foot-Foot ms^{-1}	Phase Difference ms^{-1}
20 mm	1-3	6.84	7.38
	2-3	1.95	10.50
	1-4	4.56	4.40
	2-4	1.71	-12.6
30 mm	3-6	3.80	4.30
	4-6	4.66	4.16
	3-5	4.66	1.87
	4-5	6.03	1.36
50 mm	1-6	4.62	4.53
	2-6	2.76	6.26
	1-5	5.34	2.20
	2-5	3.00	2.72

method outputs the time delay between each LED reading at the largest frequency amplitude. As shown in Figure 7, LEDs 2 and 5 have the least pronounced waveform feet.

From Table, 1 the foot to foot and the phase difference method gave results within the expected range for a select few LEDs. The waveform from LED 2 did not have a steep rise at systole, causing both methods to incorrectly estimate PWV. This incorrect phase caused the phase difference method to output that the LED 2 foot occurred after LED 4. The foot of the waveform of LED 5 was identifiable, leading to acceptable results in the foot-foot method. However, the phase difference method calculated slow PWV values outside the expected range for the same LED.

For both methods, all results from testing between LEDs 1-3, 1-4, 3-6, 4-6, 1-6 were acceptable. This acceptable set of results shows that both methods rely on a correctly shaped waveform, unlike LED 2 and LED 5.

5. DISCUSSION

While the foot-foot method gave more reliable results, the position of each foot is difficult to place, as the actual foot may occur between measurements. The time resolution of each LED is 1.75 ms, meaning that the associated variation in PWV may vary by as much as 1.5 m s^{-1}, a large possible variation in PWV. Thus, a faster sample rate is needed to improve accuracy. With a faster sample rate, the phase method is expected to perform better than the foot-foot method.

The phase difference method has the same time resolution as the foot-foot method. However, the phase is taken across the whole signal, essentially averaging the errors in each waveforms foot position. It was expected each LED plot would be the same shape, meaning the phase difference is solely because of the PWV and not the reflected wave. This assumption did not hold, as sensor pressure was different for each LED, giving different pulse shapes and amplitudes. An increase in pressure reduces the volume of blood under the sensor, reducing the pulse amplitude.

Overall, the foot-foot method gave more reliable PWV readings than the phase difference method. The phase detection method is also unable to get PWV for individual waves due to the edge effects of the FFT. In this case, the large dicrotic notch in LED 3 would lag behind systole of LED 5, instead of comparing both systole events. As signal amplitudes were varied between each LED reading, systole was less pronounced (LED 5). LED 5 had a pulse amplitude of 12 clock counts, with a resolution of 2 clock counts. These values only gave a range of 6 different values between the peak and trough of the waveform. While filtering did smooth the signal, the pulse amplitude is required to be larger to reliably give the waveform foot.

The benefit of the regional carotid-femoral PWV method is the large distance between sensors. Local measurement must occur at a faster sample rate to get the same PWV calculation reliability. At 570 Hz, the sensor was shown to estimate PWV within physiological regions. However, a sample rate of 1 kHz would improve both methods of detection. At 20 mm, 30 mm and 50 mm, a PWV of 5 m s^{-1} would result in a delay of 4 ms, 6 ms and 10 ms respectively. A benefit of this sensor is the ability to isolate the largest amplitude signal across each array. The sensor can be placed on the neck, with the carotid artery highly likely to be within the 50 mm each array spans. This means that signals such as LED 2 and LED 5 can be discarded for better signals.

A possible reason for the lower PWV at other readings is that the sensor is detecting capillary pulse rather than the carotid pulse. The elastance and thus PWV increases towards the peripheral arteries and arterioles, so the reflected wave will shift further into the forward wave, causing a different phase estimation. It is assumed that the largest pulse amplitude is from the carotid artery, which was shown in the LEDs with the largest amplitudes giving physiological PWV values.

This paper agrees with Hsu and Young (2014) that a 1 kHz should be the minimum sample rate for local PWV measurement. Even at 50 mm, the sample rate of 570 Hz was not fast enough for reliable results. Further testing with this sensor should be at a minimum of 1 kHz.

All testing was done with a distance of 5 mm between emitting and detecting LED. Increasing the distance to 10 mm will increase the time to discharge, increasing the clock count resolution. The drive current for each LED will be increased to 30 mA to reduce noise levels from ambient

light. While the ATtiny88 was able to record a pulse running at 8 MHz, using a different micro-controller that runs at 16 MHz would double the clock count resolution. As the LED decay time drives the sample rate, increasing the clock resolution will increase the accuracy of the sensor without affecting sample rate.

6. CONCLUSION

This paper described the design and testing of a pulse wave velocity (PWV) sensor to be placed on the carotid artery. Local pulse wave velocity offers improvements on the current gold standard of carotid-femoral PWV measurements. The sensor consists of three arrays of 20 LEDs placed at 5 mm increments along 50 mm. To reduce the design complexity, LEDs were used to emit and detect light, removing the need for a complex analog photodiode circuit. The arrays locate the strongest pulse signal from the carotid artery at 20 mm, 30 mm and 50 mm spacing. The sample rate of 570 Hz was fast enough to give PWV values in the region of $4\,\mathrm{m\,s^{-1}}$. However, it is recommended to use a faster sample rate as PWV may vary by $1.5\,\mathrm{m\,s^{-1}}$ using the foot-foot method. Further work on the sensor will increase the power of the LEDs, measure at 10 mm LED spacing and will sample at 1 kHz or faster.

Overall, of the two methods used to validate the sensor, the foot-foot method gave more consistent results than the phase difference method. Testing was only done on one subject. However, the accuracy of the sensor must be improved before further testing to validate against known PWV values.

REFERENCES

Balmer, J., Pretty, C., Kamoi, S., Davidson, S., Pironet, A., Desaive, T., Shaw, G.M., and Chase, J.G. (2017). Electrocardiogram R-wave is an Unreliable Indicator of Pulse Wave Initialization. *IFAC-PapersOnLine*, 50(1), 856–861.

Bertram, C., Gow, B., and Greenwald, S. (1997). Comparison of different methods for the determination of the true wave propagation coefficient, in rubber tubes and the canine thoracic aorta. *Medical Engineering & Physics*, 19(3), 212–222.

Boutouyrie, P. and Vermeersch, S. (2010). Determinants of pulse wave velocity in healthy people and in the presence of cardiovascular risk factors: 'establishing normal and reference values'. *European Heart Journal*, 31(19), 2338–2350.

Boutouyrie, P., Briet, M., Collin, C., Vermeersch, S., and Pannier, B. (2009). Assessment of pulse wave velocity. *Artery Research*, 3(1), 3–8.

Fabian, V., Matera, L., Bayerova, K., Havlik, J., Kremen, V., Pudil, J., Sajgalik, P., and Zemanek, D. (2019). Noninvasive Assessment of Aortic Pulse Wave Velocity by the Brachial Occlusion-Cuff Technique: Comparative Study. *Sensors*, 19(16), 3467.

Hsu, Y.P. and Young, D.J. (2014). Skin-Coupled Personal Wearable Ambulatory Pulse Wave Velocity Monitoring System Using Microelectromechanical Sensors. *IEEE Sensors Journal*, 14(10), 3490–3497.

Janić, M., Lunder, M., and Šabovič, M. (2014). Arterial Stiffness and Cardiovascular Therapy. *BioMed Research International*, 2014, 1–11.

Kadoglou, N.P., Papadakis, I., Moulakakis, K.G., Ikonomidis, I., Alepaki, M., Moustardas, P., Lampropoulos, S., Karakitsos, P., Lekakis, J., and Liapis, C.D. (2012). Arterial stiffness and novel biomarkers in patients with abdominal aortic aneurysms. *Regulatory Peptides*, 179(1-3), 50–54.

Kazune, S., Grabovskis, A., Strike, E., and Vanags, I. (2014). Arterial Stiffness Measured by Pulse Wave Velocity in Patients with Early Sepsis. *Proceedings of the Latvian Academy of Sciences. Section B. Natural, Exact, and Applied Sciences.*, 68(5-6), 237–241.

Kennedy, S.M. (2015). An introduction to pulse oximeters: Equations and theory. *University of Wisconsin-Madison*, 20.

Lau, K.T., Baldwin, S., O'Toole, M., Shepherd, R., Yerazunis, W.J., Izuo, S., Ueyama, S., and Diamond, D. (2006). A low-cost optical sensing device based on paired emitter–detector light emitting diodes. *Analytica Chimica Acta*, 557(1-2), 111–116.

Laurent, S., Cockcroft, J., Van Bortel, L., Boutouyrie, P., Giannattasio, C., Hayoz, D., Pannier, B., Vlachopoulos, C., Wilkinson, I., Struijker-Boudier, H., and on behalf of the European Network for Non-invasive Investigation of Large Arteries (2006). Expert consensus document on arterial stiffness: methodological issues and clinical applications. *European Heart Journal*, 27(21), 2588–2605.

Mendis, S. (2015). *Global status report on noncommunicable diseases: 2014*. World Health Organization. OCLC: 960026407.

O'Toole, M. and Diamond, D. (2008). Absorbance Based Light Emitting Diode Optical Sensors and Sensing Devices. *Sensors*, 8(4), 2453–2479.

Pereira, T., Correia, C., and Cardoso, J. (2015). Novel Methods for Pulse Wave Velocity Measurement. *Journal of Medical and Biological Engineering*, 35(5), 555–565.

Peter, L., Foltyn, J., and Cerny, M. (2015). Pulse wave velocity measurement; developing process of new measuring device. 59–62. IEEE.

Salvi, P., Magnani, E., Valbusa, F., Agnoletti, D., Alecu, C., Joly, L., and Benetos, A. (2008). Comparative study of methodologies for pulse wave velocity estimation. *Journal of Human Hypertension*, 22(10), 669–677.

Segers, P., Kips, J., Trachet, B., Swillens, A., Vermeersch, S., Mahieu, D., Rietzschel, E., De Buyzere, M., and Van Bortel, L. (2009). Limitations and pitfalls of non-invasive measurement of arterial pressure wave reflections and pulse wave velocity. *Artery Research*, 3(2), 79–88.

Shen, H., Yang, Y.H., Wu, C.C., Sune, S.T., Lee, Y.C., Lee, S.S., Zhang, W.C., Shih, Y.S., Huang, S.C., Huang, Y.C., and Chou, L.C. (2010). A novel 500 samples/sec 4 by 4 photoplethysmography (PPG) array based cosmetic chip design. In *2010 International Computer Symposium (ICS2010)*, 942–947. IEEE, Tainan, Taiwan.

Sorensen, G.L., Jensen, J.B., Udesen, J., Holfort, I.K., and Jensen, J.A. (2008). Pulse wave velocity in the carotid artery. In *2008 IEEE Ultrasonics Symposium*, 1386–1389. IEEE, Beijing, China.

Stojanovic, R. and Karadaglic, D. (2013). Design of an Oximeter Based on LED-LED Configuration and FPGA Technology. *Sensors*, 13(1), 574–586.